

# Structure, Spectral and Photocatalytic Properties of Self-Doped $\text{TiO}_{2-x}$ Thin Films

Jin Yaxue<sup>1,2</sup>, Wang Bin<sup>1</sup>, Qi Hongji<sup>1</sup>, Zhu Maodong<sup>1</sup>

<sup>1</sup> Key Laboratory of Materials for High Power Laser, Shanghai Institute of Optics and Fine Mechanics, Chinese Academy of Sciences, Shanghai 201800, China; <sup>2</sup> University of Chinese Academy of Sciences, Beijing 100049, China

**Abstract:** The titanium dioxide thin films (TTFs) were prepared by the electron beam evaporation system and annealed in air and  $\text{H}_2$ . With excellent stability, samples annealed in  $\text{H}_2$  maintain their pale yellow in the air for nearly one year. The structure, morphology, spectral and photocatalytic properties of TTFs were observed and discussed. The results show that titanium oxide films annealed in  $\text{H}_2$  have better catalytic performance than those annealed in air.  $\text{Ti}^{3+}$  can improve photocatalytic efficiency since the electronic structures of TTFs annealed in  $\text{H}_2$  can be finely tuned by the doped  $\text{Ti}^{3+}$ . The existence of  $\text{Ti}^{3+}$  induces an electronic band below the conduction band and narrows the band gap.

**Key words:** self-doped  $\text{TiO}_{2-x}$  thin film; materials characterization; photocatalytic activity

As the promising semiconductor material, titanium dioxide ( $\text{TiO}_2$ ) with the large availability, non-toxicity, high chemical stability and low cost, has attracted a lot of researchers in optical, electrical and photoelectrochemical applications<sup>[1-4]</sup>. However, its wide band gap (3.2 eV for anatase) limits the photocatalytic efficiency of  $\text{TiO}_2$ <sup>[5]</sup>. Therefore, tremendous methods have been proposed to control the band-gap of  $\text{TiO}_2$ , making it sensitive to visible light.

In recent years, self-doped titanium oxide film ( $\text{TiO}_{2-x}$ )<sup>[6-8]</sup> has been researched as an interesting material to increase the visible light absorption due to localized oxygen vacancy states<sup>[7]</sup>. Unlike other doping methods<sup>[9,10]</sup>, self-doping avoids other impurity elements being introduced<sup>[11]</sup>, which should be beneficial for preserving the  $\text{TiO}_2$  intrinsic phase and results in the low recombination during photocatalytic process. With  $\text{Ti}^{3+}$  and oxygen vacancies being doped, both visible-light photocatalytic activities of anatase and rutile phases have been improved.

In the present paper, titanium dioxide thin film (TTF) has been fabricated by electron beam evaporation system and annealed in air and  $\text{H}_2$  to improve the crystallinity and get the  $\text{Ti}^{3+}$  doped ions. The structure, morphology, spectral and

photocatalytic properties of TTFs have been observed and discussed.  $\text{TiO}_{2-x}$  thin films annealed in  $\text{H}_2$  have better catalytic performance, which can be attributed to the enhanced  $\text{Ti}^{3+}$  content. Based on the systematical research, it is concluded that the  $\text{Ti}^{3+}$  content in samples could increase the photocatalytic efficiency.

## 1 Experiment

The TTFs were deposited in electron beam evaporation system. Before deposition, the quartz glass substrate was ultrasonic cleaned in acetone and ethanol for 0.5 h. Depositions of the TTFs were carried out at the total pressure of  $2 \times 10^{-3}$  Pa, and the pure oxygen was used as carrier gas with a gas flow rate of 200 mL/min. Granular  $\text{TiO}_2$  was evaporated to the substrate surface 27 cm away from the evaporation source, and substrate rotation and 6 kV high voltage were set. After the deposition, TTFs were annealed under the corresponding atmosphere in a muffle furnace to improve crystallization (in air) and produce the self-doped  $\text{TiO}_{2-x}$  thin films (in  $\text{H}_2$ ). For setting the contrast experimental results, four samples were produced for heat treatment of different conditions. The detailed process is listed in Table 1.

Received date: December 20, 2018

Foundation item: National Natural Science Foundation of China (11535010)

Corresponding author: Wang Bin, Ph. D., Key Laboratory of Materials for High Power Laser, Shanghai Institute of Optics and Fine Mechanics, Chinese Academy of Sciences, Shanghai 201800, P. R. China, Tel: 0086-21-69918478, E-mail: wangbinmars@siom.ac.cn

Copyright © 2019, Northwest Institute for Nonferrous Metal Research. Published by Science Press. All rights reserved.

**Table 1 Detailed annealing conditions for TTFs**

Sample No.	Annealing condition
TTF as-grown	As-deposition
TTF 400 °C	400 °C, 2 h, in air
TTF 450 °C	450 °C, 2 h, in air
TTF 400 °C H <sub>2</sub>	400 °C, 2 h, in H <sub>2</sub>
TTF 450 °C H <sub>2</sub>	450 °C, 2 h, in H <sub>2</sub>

The photocatalytic capacity of TTFs was measured by the decomposition of methylene blue (MB) solution with exterior irradiation at the room temperature. For photocatalytic reaction, a 300 W high pressure Xe lamp with an ultraviolet cutoff filter to block ultraviolet region light was used as a light source; 10 mg MB was dispersed into 10 mL of 10 mg/L MB solution. Before irradiation, the solution was magnetically stirred in the dark for 2 h to ensure the absorption/desorption balance of photocatalyst and MB, and then the mixture was stirred constantly under the light at 200 mm distance. The MB degradation was characterized by measurement of the dye absorption change at 620 nm with a 30 min interval.

## 2 Results and Discussion

### 2.1 Structure analysis

Fig.1a shows the X-ray diffraction (XRD) patterns of TTFs. The TiO<sub>2</sub> film annealed at 300 °C in air mainly contains the anatase phase<sup>[12]</sup>. The average grain sizes of TTFs after 400 and 450 °C annealing in air are 11.8 and 13.8 nm, respectively, and the higher annealing temperature results in the larger crystal size. However, the XRD pattern of TTF 400 °C H<sub>2</sub> shows several broad and weak anatase peaks. Compared with TTF 400 °C H<sub>2</sub>, TTF 450 °C H<sub>2</sub> exhibits the higher crystallization with 9.6 nm crystal size, which means the higher annealing temperature in H<sub>2</sub> improves cooperative atom diffusion resulting in the higher crystallization. Simultaneously, TTF 450 °C H<sub>2</sub> shows a crystal preferential orientation of anatase (101), different from TTFs annealed in air (004). During the cooling process, a nucleation region resulting from the cooperative atom movements could be accompanied by the high symmetry crystal phase transforming into the lower symmetry phase. This process could occur in different ways with some randomness. Therefore, different atmosphere can lead to different preferential orientations.

Fig.1b shows the Raman spectra of TTFs. The as-grown TTF shows a very weak Raman peak, showing an amorphous structure. After annealing, the vibration peaks of 143, 395, 515, 519 (superposition with 515 cm<sup>-1</sup> line) and 638 cm<sup>-1</sup> were E<sub>g</sub>, B<sub>1g</sub>, B<sub>1g</sub>, A<sub>1g</sub>, and E<sub>g</sub>, respectively, consistent with the Refs. [13,14]. The existence of the 143 cm<sup>-1</sup> model shows that TTF 400 °C and TTF 450 °C have a certain degree of anatase phase<sup>[15]</sup>. The broad and weak 143 cm<sup>-1</sup> Raman peak of TTF 400 °C H<sub>2</sub> shows low crystallinity, and the Raman peak intensity of TTF 450 °C H<sub>2</sub> is higher than that of TTF 400 °C H<sub>2</sub>. Compared with the Raman peaks of TTF 400 °C and

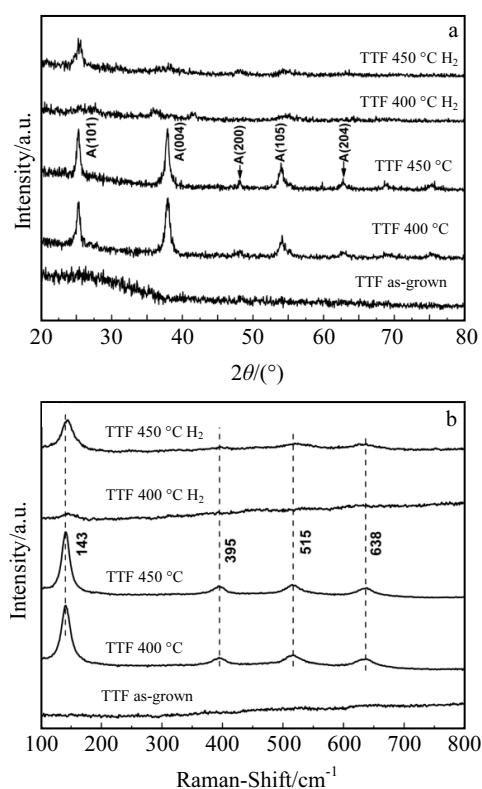


Fig.1 XRD patterns (a) and Raman spectra (b) of TTFs under different annealing conditions

450 °C, Raman lines of TTFs annealed in H<sub>2</sub> exhibit the weak and broad feature, which shows the structural disorder with imperfect nanocrystals. The large blue shift of Raman peak can be seen in TTFs annealed in H<sub>2</sub>. Similar to previous reports, phonon confinement resulting from finite grains size (9.6 nm) and the existence of defects (oxygen vacancies) cause the blue-shift of Raman peak.

### 2.2 Optical properties and morphology analysis

Fig.2 is the transmission spectra of the TTFs. The transmittance edges of TTFs get red-shifted after annealing, showing a decrease in the band gap. The similar phenomenon can be found in the Refs. [16,17]. The phenomenon can be ascribed to scattering and absorption increase in TTFs after annealing treatment. Under high temperature annealing conditions, oxygen of TTFs would release to environment so that the oxygen vacancy content would increase in TTFs during the annealing process<sup>[18]</sup>. Another reason is that the surface has a higher scattering loss with the annealing temperature increase.

Fig.3 shows the 3D morphological insets of TTFs annealed under different conditions. The surface roughness of TTFs increases with the annealing temperature increasing, despite of close roughness values. Simultaneously, the roughness value of TTF annealed in air is higher than that of TTF annealed in H<sub>2</sub> at the same temperature. This may be because oxygen in

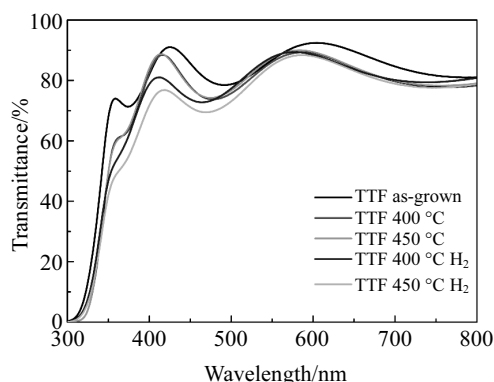


Fig.2 Transmission spectra of TTFs under different thermal treatment conditions

air promotes atomic diffusion and grain growth. In addition, the close roughness values of TTFs with different treatments could guarantee that the influence of surface roughness on the photocatalytic activity is almost the same.

### 2.3 Chemical state

Fig.4 shows the XPS spectra of TTFs. It was studied using the peak of C1 (284.6 eV) of surface organic pollutants as calibration reference. Only 458.73 eV  $Ti^{4+} 2p_{3/2}$  peak for TTF as-grown is shown in the Ti 2p XPS spectra of Fig.4. Compared with TTF as-grown, the movement of Ti 2p core peak to low binding energy for TTFs after annealing in air indicates the existence of  $Ti^{3+}$ [19, 20]. The offset value of Ti 2p core peak rises with the annealing temperature increasing. The obvious 0.51 eV binding energy offset of TTF 450 °C is observed. As shown in Fig.4, the O 1s of 530.24 eV peaks for TTF as-grown is shown in the O 1s XPS spectra. Just like the shift phenomenon of Ti 2p peak, the shift to lower binding energy side of O 1s core level peaks for TTFs annealed in air are also observed. The binding energy offset of O 1s for TTF 450 °C reaches to 0.69 eV. The amount shift of O 1s peak highlights the oxygen-deficient state for samples annealed above 400 °C, which could influence the material chemical properties. However, Ti  $2p_{3/2}$  located at 458.56 eV and O 1s located at 530.27 eV for TTFs annealed in  $H_2$  are assigned to

$Ti^{4+}$  in  $TiO_2$ . The XPS data indicate that there is no  $Ti^{3+}$  present on the surface of TTFs annealed in  $H_2$ , and it is believed that surface  $Ti^{3+}$  of TTFs annealed in  $H_2$  as the more unstable structure than that of TTF annealed in air would tend to adsorb atmosphere  $O_2$  more easily and become nearly stoichiometric. Compared with the transmission spectrum, we further confirm the conclusion that  $Ti^{3+}$  of TTFs annealed in  $H_2$  exists in the bulk. The conclusion is consistent with other researches about self-doped  $TiO_{2-x}$  annealed in reduced atmosphere that the nearly stoichiometric surface of  $TiO_{2-x}$  could preserve the nanocrystal core from further oxidation.

### 2.4 Discussion of PL properties

Fig.5 is the photoluminescence spectroscopy (PL) of the TTFs. The weak transmitting band from 350 nm to 380 nm can be attributed to the band edge transition luminescence[21,22]. Even the diameter size of  $TiO_2$  nanoparticles rises after annealing; weak band edge luminescence indicates the existence of defects during annealing process. As expected, the 410~470 nm emission band of TTFs decreases after annealing due to the improvement of crystal quality. As previously reported[23], the 500~650 nm emission band centered at 565 nm is close to 560 nm. After the vacuum treatment, the increase of oxygen vacancy may lead to the green emission of 560 nm traps[24,25].

### 2.5 Photocatalytic activity

Fig.6 shows  $\ln(C_0/C_t)$  vs  $t$  (time) profiles with the visible light irradiation for MB aqueous solution degradation, where  $C_0$  is the MB concentration after photocatalysts absorption equilibrium before irradiation and  $C_t$  is the MB concentration at irradiation time  $t$ . The stability of the TTFs was confirmed by the linear relationship of  $\ln(C_0/C_t)$  vs  $t$ [26]. Table 2 shows the calculated kinetic constants ( $k/\text{min}^{-1}$ ). After annealing in air, the kinetic constant shows an increase, the line slope of TTF 450 °C shows 2 times higher than that of TTF as-grown. Obviously, more anatase titanium phase in TTF 450 °C results in faster degradation of MB. Although  $Ti^{3+}$  and oxygen vacancies of TTF 400 °C  $H_2$  could favor the photocatalytic activity, and the photodegradation efficiency of TTF 400 °C  $H_2$  is comparable to that of TTF 450 °C, in view of the lower crystallization. With the increase in oxygen vacancies and

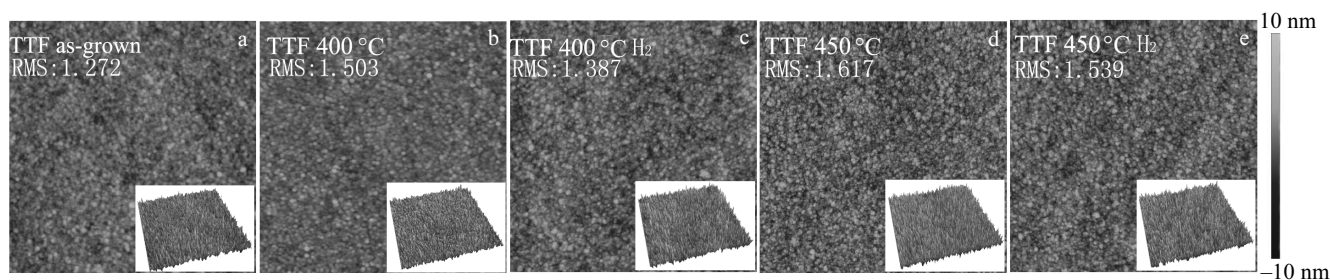


Fig.3 AFM characterization of  $2.5 \mu\text{m} \times 2.5 \mu\text{m}$  images and the 3D morphological insets of TTFs annealed under different conditions: (a) TTF as-grown, (b) TTF 400 °C, (c) TTF 400 °C  $H_2$ , (d) TTF 450 °C, and (e) TTF 450 °C  $H_2$

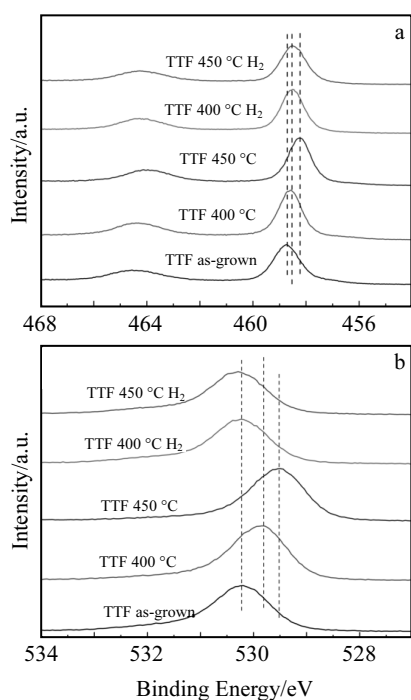


Fig.4 Ti 2p (a) and O 1s (b) spectra of TTFs under different annealing conditions

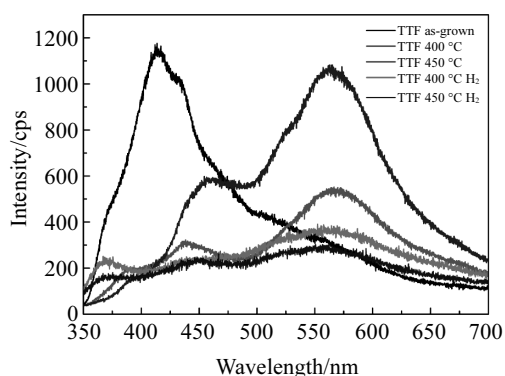


Fig.5 Emission spectra of TTFs under different annealing conditions

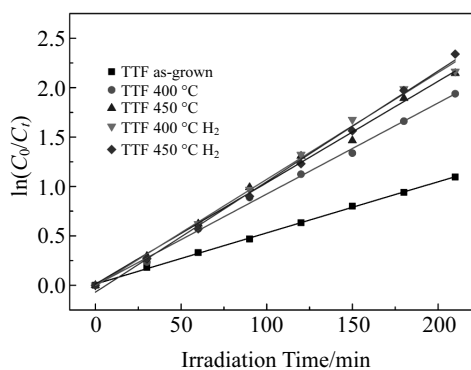


Fig.6 Photodegradation of MB by TTFs under different annealing conditions

Table 2 Kinetic constant ( $k$ ) of MB photodegradation

Sample No.	TTF as-grown	TTF 400 °C	TTF 450 °C	TTF 400 °C H <sub>2</sub>	TTF 450 °C H <sub>2</sub>
$k/ \times 10^{-3} \text{ min}^{-1}$	5.2	9.2	10.2	10.6	11.3

Ti<sup>3+</sup>, the kinetic constant of TTF 450 °C H<sub>2</sub> reaches  $1.13 \times 10^{-2} \text{ min}^{-1}$ , showing superior photocatalytic performance. Obviously, after 450 °C annealing, Ti<sup>3+</sup> and oxygen vacancy play a major role.

### 3 Conclusions

1) Amorphous TTFs were fabricated by electron beam evaporation system and annealed in H<sub>2</sub> and air to increase crystallinity and get Ti<sup>3+</sup>.

2) TiO<sub>2-x</sub> thin films annealed in H<sub>2</sub> have better catalytic performance than those annealed in air.

3) The photocatalytic kinetic constant of TTF 450 °C H<sub>2</sub> reaches  $1.13 \times 10^{-2} \text{ min}^{-1}$ , and the Ti<sup>3+</sup> and oxygen vacancies play a key role in the catalytic process.

4) The Ti<sup>3+</sup> in samples could narrow the band gap by tuning the electronic structures of TTFs annealed in H<sub>2</sub> to control the photocatalytic efficiency.

### References

- Hoang S, Guo S, Mullins C B. *The Journal of Physical Chemistry C*[J], 2012, 116(44): 23 283
- Lee K, Schmuki P. *Electrochemistry Communications*[J], 2012, 25: 11
- Fu K, Huang J, Yao N et al. *Industrial & Engineering Chemistry Research*[J], 2015, 54(2): 659
- Wu Binbin, Pan Fengming, Yang Yu'e. *Chinese Physics Letters*[J], 2011, 28(11): 118 102
- Nakata K, Fujishima A. *Journal of Photochemistry and Photobiology C: Photochemistry Reviews*[J], 2012, 13(3): 169
- Chen X B, Liu L, Peter Y Y et al. *Science*[J], 2011, 331(6018): 746
- Zuo F, Wang L, Wu T et al. *Journal of the American Chemical Society*[J], 2010, 132(34): 11 856
- Sasikala R, Sudarsan V, Sudakar C et al. *International Journal of Hydrogen Energy*[J], 2009, 34(15): 6105
- Zheng J, Liu Z Q, Liu X et al. *Journal of Alloys and Compounds*[J], 2011, 509(9): 3771
- Juma A, Acik I O, Oluwabi A T et al. *Applied Surface Science*[J], 2016, 387: 539
- Zhu Q, Peng Y, Lin L et al. *Journal of Materials Chemistry A*[J], 2014, 2(12): 4429
- Nakamura T, Ichitsubo T, Matsubara E et al. *Scripta Materialia*[J], 2005, 53(9): 1019
- Zhang J, Li M J, Feng Z C et al. *The Journal of Physical Chemistry B*[J], 2006, 110(2): 927
- Mikami M, Nakamura S, Kitao O et al. *Physical Review B*[J], 2002, 66(15): 155 213

- 15 Zhang W F, Zhang M S, Yin Z et al. *Applied Physics B*[J], 2000, 70(2): 261
- 16 Wang B, Qi H J, Wang H et al. *Optical Materials Express*[J], 2015, 5(6): 1410
- 17 Won D J, Wang C H, Jang H K et al. *Applied Physics A*[J], 2001, 73(5): 595
- 18 Tian G L, Dong L, Wei C Y et al. *Optical Materials*[J], 2006, 28(8-9): 1058
- 19 Kang S H, Kim J Y, Kim Y et al. *The Journal of Physical Chemistry C*[J], 2007, 111(26): 9614
- 20 Wang B, Qi H J, Chai Y J et al. *Superlattices and Microstructures*[J], 2016, 90: 87
- 21 Pan D, Zhao N, Wang Q et al. *Advanced Materials*[J], 2005, 17(16): 1991
- 22 Liu Y J, Claus R O. *Journal of the American Chemical Society*[J], 1997, 119(22): 5273
- 23 Knorr F J, Zhang D, McHale J L. *Langmuir*[J], 2007, 23(17): 8686
- 24 McHale J L, Rich C C, Knorr F J. *MRS Online Proceedings Library Archive*[J], 2010, 1268: EE03
- 25 Mercado C C, Knorr F J, McHale J L et al. *The Journal of Physical Chemistry C*[J], 2012, 116(19): 10 796
- 26 Jiang X, Zhang Y, Jiang J et al. *The Journal of Physical Chemistry C*[J], 2012, 116(42): 22 619

## 自掺杂二氧化钛薄膜的结构、光谱和光催化性能

靳亚雪<sup>1,2</sup>, 王 斌<sup>1</sup>, 齐红基<sup>1</sup>, 朱茂东<sup>1</sup>

(1. 中国科学院 上海光学精密机械研究所 强激光材料重点实验室, 上海 201800)

(2. 中国科学院大学, 北京 100049)

**摘 要:** 采用电子束蒸发系统制备氧化钛薄膜并分别在氢气和空气中退火, 在氢气中退火的样品由于其稳定性强, 能在空气中保持淡黄色将近一年。对氧化钛薄膜的结构, 形貌, 光谱和光催化性能进行详细讨论。结果表明, 在氢气中退火的薄膜比在空气中退火的薄膜具有更好的光催化性能, 氢气中退火的样品通过  $\text{Ti}^{3+}$  掺杂能很好地调控电子结构从而提高光催化效率。 $\text{Ti}^{3+}$  的存在缩小了带隙。

**关键词:** 自掺杂二氧化钛薄膜; 材料特征; 光催化性能

---

作者简介: 靳亚雪, 女, 1992 年生, 硕士生, 中国科学院上海光学精密机械研究所强激光材料重点实验室, 上海 201800, E-mail: 363955335@qq.com